PNAS Nexus

PNAS Nexus, 2022, **2**, 1–12
https://doi.org/10.1093/pnasnexus/pgac297
Advance access publication date: 16 December 2022
Research Report

Topical SCD-153, a 4-methyl itaconate prodrug, for the treatment of alopecia areata

Jerry Tsai [a], Sadakatali Gori [b], Jesse Alt [b], Sandhya Tiwari[c], Jitesh Iyer[c], Rashmi Talwar[c], Denish Hinsu[d], Kailash Ahirwar[e], Swayam Mohanty[d], Chintan Khunt[d], Brijesh Sutariya [f], Kaushal Jani[d], Venkatesha Venkatasubbaiah[d], Ashok Patel[g], Jasmin Meghapara[g], Kaushal Joshi[g], Rajanikanta Sahu[g], Vijay Rana[g], Prashant Nigade[g], Ravi S. Talluri[h], Kadiyala V.S.N. Murty[i], Kiritkumar Joshi[i], Vikram Ramanathan[j], Ang Li [a], Nasif Islam [a], Ivan Snajdr [k], Pavel Majer[k], Rana Rais [b,l,m,*], Barbara S. Slusher [b,l,m,n,o,p,q,*] and Luis A. Garza [a,q,r,*]

[a]Department of Dermatology, Johns Hopkins University School of Medicine, Baltimore, MD 21205, USA
[b]Johns Hopkins Drug Discovery, Johns Hopkins University School of Medicine, Baltimore, MD 21205, USA
[c]In Vitro Biology, Sun Pharma Advanced Research Company, Savli, 391770, India
[d]Preclinical Pharmacology, Sun Pharma Advanced Research Company, Savli, 391770, India
[e]Department of Pharmaceutics, National Institute of Pharmaceutical Education and Research Ahmedabad, Gandhinagar 382355, India
[f]Department of Internal Medicine, Division of Hematology/Oncology, University of Iowa, Iowa City, IA 52242, USA
[g]Drug Metabolism and Pharmacokinetics, Sun Pharma Advanced Research Company, Savli, 391770, India
[h]Clinical Pharmacology, Sun Pharma Advanced Research Company, Mahakali, Mumbai 400093, India
[i]Medicinal Chemistry, Sun Pharma Advanced Research Company, Savli 391770, India
[j]Translational Development, Sun Pharma Advanced Research Company, Savli 391770, India
[k]Institute of Organic Chemistry and Biochemistry, Academy of Sciences of the Czech Republic v.v.i., Prague 166 10, Czech Republic
[l]Department of Neurology, Johns Hopkins University School of Medicine, Baltimore, MD 21205, USA
[m]Department of Pharmacology and Molecular Sciences, Johns Hopkins University School of Medicine, Baltimore, MD 21205, USA
[n]Department of Medicine, Johns Hopkins University School of Medicine, Baltimore, MD 21205, USA
[o]Department of Psychiatry and Behavioral Sciences, Johns Hopkins University School of Medicine, Baltimore, MD 21205, USA
[p]Department of Neuroscience, Johns Hopkins University, Baltimore, MD 21205, USA
[q]Department of Oncology, Johns Hopkins University School of Medicine, Baltimore, MD 21205, USA
[r]Department of Cell Biology, Johns Hopkins University, Baltimore, MD 21205, USA
*To whom correspondence should be addressed: Email: rrais2@jhmi.edu, bslusher@jhmi.edu, lag@jhmi.edu
Edited By: Karsten Hiller

Abstract

Alopecia areata is a chronic hair loss disorder that involves autoimmune disruption of hair follicles by $CD8^+$ T cells. Most patients present with patchy hair loss on the scalp that improves spontaneously or with topical and intralesional steroids, topical minoxidil, or topical immunotherapy. However, recurrence of hair loss is common, and patients with extensive disease may require treatment with oral corticosteroids or oral Janus kinase (JAK) inhibitors, both of which may cause systemic toxicities with long-term use. Itaconate is an endogenous molecule synthesized in macrophages that exerts anti-inflammatory effects. To investigate the use of itaconate derivatives for treating alopecia areata, we designed a prodrug of 4-methyl itaconate (4-MI), termed SCD-153, with increased lipophilicity compared to 4-MI (CLogP 1.159 vs. 0.1442) to enhance skin and cell penetration. Topical SCD-153 formed 4-MI upon penetrating the stratum corneum in C57BL/6 mice and showed low systemic absorption. When added to human epidermal keratinocytes stimulated with polyinosinic-polycytidylic acid (poly I:C) or interferon (IFN)γ, SCD-153 significantly attenuated poly I:C-induced interleukin (IL)-6, Toll-like receptor 3, IL-1β, and IFNβ expression, as well as IFNγ-induced IL-6 expression. Topical application of SCD-153 to C57BL/6 mice in the resting (telogen) phase of the hair cycle induced significant hair growth that was statistically superior to vehicle (dimethyl sulfoxide), the less cell-permeable itaconate analogues 4-MI and dimethyl itaconate, and the JAK inhibitor tofacitinib. Our results suggest that SCD-153 is a promising topical candidate for treating alopecia areata.

Keywords: alopecia areata, hair growth, topical, itaconate, prodrug, inflammation, immunosuppression, cytokine, interleukin, interferon, double-stranded RNA, polyinosinic–polycytidylic acid, hair cycle, anagen, telogen, keratinocyte, stability, pharmacokinetics, cytotoxicity

OXFORD UNIVERSITY PRESS

Competing Interest: Authors L.G., B.S.S., P.M., N.I., and R.R. are listed as inventors in patent applications filed by Johns Hopkins Technology Ventures covering novel compositions of itaconate prodrugs inhibitors, including SCD-153, and their utility. This arrangement has been reviewed and approved by the Johns Hopkins University in accordance with its conflict of interest policies. Other authors declare that no conflicts of interest exist.
Received: July 29, 2022. **Accepted:** December 15, 2022

Significance Statement:

Itaconate is an endogenous molecule synthesized by macrophages with anti-inflammatory effects. This study examined the stability, pharmacokinetics, cytotoxicity, immunomodulatory activity, and potential for hair induction of topical SCD-153, a 4-methyl itaconate (4-MI) prodrug with increased lipophilicity for enhanced skin and cell penetration. SCD-153 attenuated the expression of proinflammatory mediators in human epidermal keratinocytes. Topical application of SCD-153 to C57BL/6 mice in the resting phase of the hair cycle induced significantly more hair growth than 4-MI, dimethyl itaconate, and tofacitinib. This study suggests that itaconate derivatives may serve as a first-in-class topical treatment for alopecia areata and fill unmet needs in current management strategies.

Introduction

Alopecia areata is a chronic nonscarring hair loss disorder that affects 2 in 100 individuals globally and has increased in prevalence over the past decades (1). Its pathogenesis involves the loss of immune privilege and autoimmune attack of hair follicles by $CD8^+$ T cells (2, 3). While patients with alopecia areata typically present with recurrent patchy hair loss on the scalp, around 5% of patients progress to complete hair loss on the scalp (alopecia totalis) or throughout the body (alopecia universalis) (4). Nearly 70% of patients with limited scalp involvement tend to experience complete hair regrowth, but those with extensive disease may worsen over time (5) and develop irreversible hair loss if the condition persists for more than 10 years (6). Due to its chronic and potentially refractory nature, alopecia areata is associated with a significant psychological burden and negative quality of life (7, 8).

Various treatments are used to mitigate hair loss and accelerate hair regrowth in alopecia areata, such as corticosteroids (topical, intralesional, and oral), topical minoxidil, and topical immunotherapy (e.g., diphenylcyclopropenone, squaric acid dibutylester), but none have been shown to have lasting benefit (9). Oral corticosteroids may be used in patients with extensive or treatment-resistant alopecia areata, but their disruption of immune, metabolic, and endocrine functions make them unsuitable for long-term use. The recent discovery of Janus kinase (JAK)-signal transducer and activator of transcription (STAT) signaling in the pathogenesis of alopecia areata has led to the successful management of patients with severe condition using oral JAK inhibitors (e.g., ruxolitinib, tofacitinib) (3, 10–12). However, disease recurrence after discontinuation of oral JAK inhibitors remains a challenge, and their long-term use must be weighed against the potential side effects of infections, marrow suppression, transaminitis, and lipid abnormalities (11–13). Topical application of JAK inhibitors has been proposed as a strategy for long-term maintenance treatment, but preliminary studies have not shown significant efficacy, likely due to insufficient skin penetration of existing JAK inhibitors (11, 12).

Itaconate is an endogenous molecule synthesized by mitochondrial *cis*-aconitate decarboxylase in macrophages when stimulated by Toll-like receptor (TLR) ligands such as lipopolysaccharides (LPS), the synthetic double-stranded RNA analogue polyinosinic-polycytidylic acid (poly I:C), and type I and type II interferons (IFNs) (14). Itaconate accumulates intracellularly within activated macrophages and is also secreted to extracellular space (15, 16), and it has gained significant interest for its anti-inflammatory, antimicrobial, and antiviral effects (17). Due to the polar structure of itaconate as a dicarboxylic acid, esterified derivatives such as dimethyl itaconate (DMI), 4-octyl itaconate (4-OI), and 4-ethyl itaconate (4-EI) have been used as cell-permeable surrogates of itaconate to study downstream pathways following their exogenous administration (16, 18–21). For example, itaconate and its derivatives have been found to inhibit activation of the NOD-like receptor pyrin domain containing 3 (NLRP3) inflammasome and resulting secretion of the proinflammatory cytokine interleukin (IL)-1β (19–22). DMI and 4-OI strongly activate the nuclear factor erythroid 2-related factor 2 (NRF2)-driven electrophilic stress response and reduce proinflammatory IL-6 secretion through inhibition of the inhibitor of nuclear factor kappa B zeta (IκBζ)-activating transcription factor (ATF3) axis (19–21), whereas endogenous itaconate may downregulate IL-6 through NRF2- and ATF3-independent mechanisms (23). 4-OI inhibits LPS-induced upregulation of IFNβ, whereas endogenous itaconate augments this (21). Despite variations in their downstream effects likely owing to differing moieties and electrophilicity (21), the immunomodulatory qualities of itaconate and its derivatives have made them promising pharmacologic candidates for the treatment of inflammatory conditions like psoriasis, rheumatoid arthritis, systemic lupus erythematosus, and multiple sclerosis (14, 18, 24).

We hypothesize that itaconate-based molecules may provide therapeutic benefit in the context of alopecia areata by responding to the immune stimulants poly I:C and IFNγ, which have been suggested to contribute to the pathogenesis of alopecia areata through activation of NLRP3 inflammasome activity (25, 26) and JAK-STAT signaling (3, 27–29), respectively. The ability of itaconate and its derivatives to suppress downstream proinflammatory cytokines like IL-6, itself an activator of JAK-STAT signaling (30), as well as IL-1β, which disrupts hair cycling and is upregulated in alopecia areata scalp lesions (31–33), also presents potential mechanisms to promote hair growth. Due to its highly charged nature, itaconate does not adequately penetrate the skin barrier when applied topically. To overcome this limitation, we designed and synthesized a topical cell-permeable prodrug of 4-methyl itaconate (4-MI), SCD-153, with enhanced lipophilicity for skin penetration (CLogP 1.159 vs. 0.1442) and the ability to form 4-MI intracellularly within the epidermis and dermis. We found that SCD-153 inhibits poly I:C-induced upregulation of IL-6, TLR3, IL-1β, and IFNβ, as well as IFNγ-induced upregulation of IL-6 in human epidermal keratinocytes. We also induced significant and consistent hair growth in telogen C57BL/6 mice with topical SCD-153.

Results

SCD-153 forms 4-MI in skin homogenate and plasma

SCD-153 was synthesized using the scheme shown in Fig. 1a and has increased lipophilicity compared to 4-MI (CLogP 1.159 vs. 0.1442). SCD-153 remained stable in the solid state at room temperature with negligible change in composition after 84 days (Fig. 1b). In contrast, SCD-153 completely metabolized within 30 minutes of incubation in either mouse skin homogenate, mouse

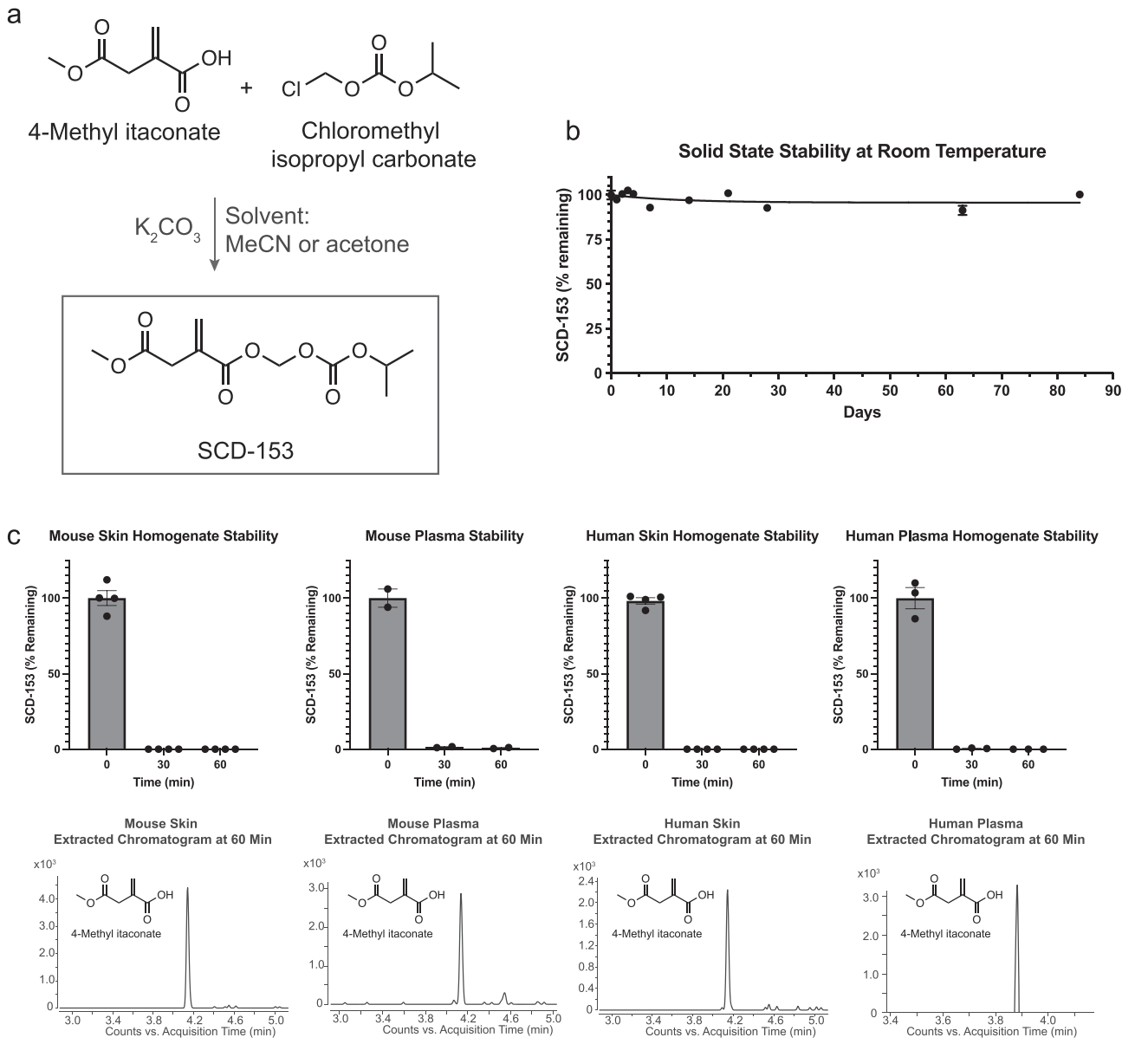

Fig. 1. SCD-153 exhibits solid-state stability at room temperature and forms 4-MI in skin homogenate and plasma. (a) The synthetic scheme of SCD-153, a prodrug of 4-MI with enhanced lipophilicity (CLogP 1.159 vs. 0.1442) for improved skin and cell penetration. (b) SCD-153 remained stable in the solid state within error of 100% after 84 days at room temperature ($n = 2$ per time point). (c) SCD-153 readily converted to 4-MI in mouse skin homogenate ($n = 4$ per time point), mouse plasma ($n = 2$ per time point), human skin homogenate ($n = 4$ per time point), and human plasma ($n = 3$ per time point). Chromatograms show the presence of significant 4-MI levels at 60 minutes after the addition of SCD-153 to skin homogenate or plasma. Data are expressed as mean ± SEM.

plasma, human skin homogenate, or human plasma, showing formation of 4-MI subsequently measured using high-resolution mass spectrometry (Fig. 1c). De-esterified itaconate was not detected in mouse and human skin homogenates at any of the time points using high-resolution mass spectrometry (Table S1).

Topically absorbed SCD-153 forms 4-MI within the epidermis and dermis

The pharmacokinetic profile of SCD-153 was studied through topical application of 5% SCD-153 in dimethyl sulfoxide (DMSO) to C57BL/6 mice, followed by measurement of SCD-153 and 4-MI concentrations in the skin and plasma, using formic acid as the stabilizer to prevent ex vivo degradation of SCD-153 (Fig. 2a). Area under the curve (AUC) values showed that cumulative exposure of SCD-153 in plasma over 24 hours was negligible compared to that of skin (0 vs. 4,345 h∗μM). Similarly, cumulative exposure of 4-MI in plasma over 24 hours was <20% to that of skin (295 vs. 1,872 h∗μM). Within the skin, 4-MI levels peaked and declined faster than SCD-153, which remained elevated (around 200 μM) even at 24 hours after application (Fig. 2a).

To better characterize the pharmacokinetics and localization of SCD-153 and 4-MI within specific skin compartments, we repeated measurements in another set of C57BL/6 mice treated with topical 5% SCD-153, using tape stripping to separate the stratum corneum from the rest of the epidermis and dermis (Fig. 2b). Measurements of SCD-153 and 4-MI levels up to 336 hours after topical application showed that SCD-153 was predominantly localized to the stratum corneum, with more than 650-fold greater maximum concentration (17,717 vs. 27 μM) and AUC over 336

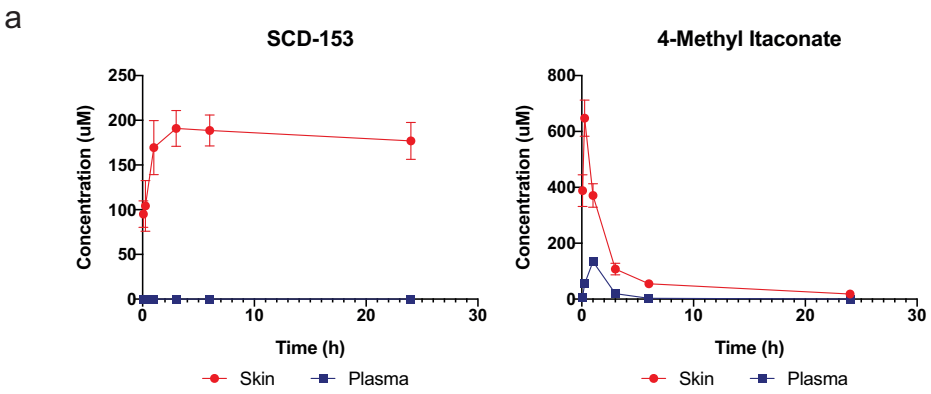

Analyte	Matrix	T_{max} (h)	C_{max} (μM)	$AUC_{0\text{-}24h}$ (h*μM)
SCD-153	Plasma	-	0	0
	Skin	3.0	191	4345
4-Methyl Itaconate	Plasma	1.0	135	295
	Skin	0.25	648	1872

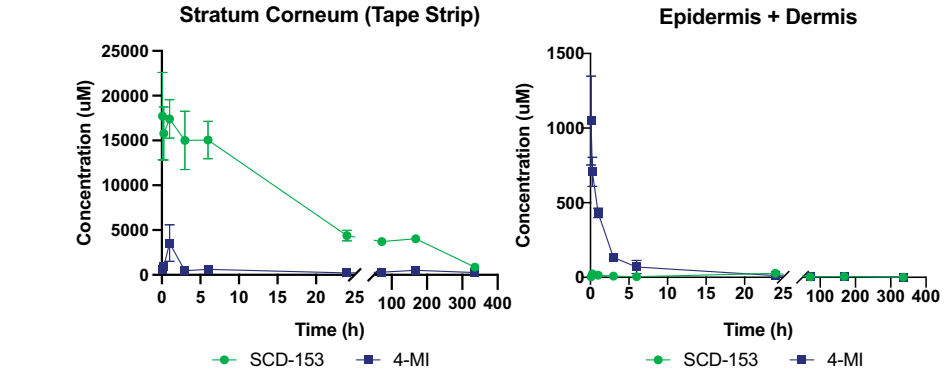

Analyte	Matrix	T_{max} (h)	C_{max} (μM)	$AUC_{0\text{-}24h}$ (h*μM)	$AUC_{0\text{-}336h}$ (h*μM)
SCD-153	Plasma	-	0	0	0
	Stratum Corneum	0.08	17717	268491	1246864
	Epidermis + Dermis	24	27	331	1868
4-Methyl Itaconate	Plasma	1.0	140	299	295
	Stratum Corneum	1.0	3543	14854	131744
	Epidermis + Dermis	0.083	1051	2218	3604

Fig. 2. SCD-153 shows minimal systemic absorption and forms 4-MI in the epidermis and dermis of C57BL/6 mice. (a) Following topical application of 5% SCD-153 in DMSO to C57BL/6 mice, levels of SCD-153 and its metabolite 4-MI were significantly higher in the skin than in the plasma ($n = 3$ per time point). (b) Levels of SCD-153 were significantly higher in the stratum corneum than in the rest of the epidermis and dermis, while 4-MI was the predominant form of the drug present in the epidermis and dermis (n = 3 per time point). Data are expressed as mean ± SEM.

hours (1,246,864 vs. 1,868 h$*\mu$M) in the stratum corneum compared to the rest of the epidermis and dermis. 4-MI was the predominant form of the drug present within the epidermis and dermis, with a maximum concentration of 1,051 μM at 5 minutes after treatment that decreased exponentially and approached zero by 24 hours after treatment (Fig. 2b).

SCD-153 inhibits immune activation in human eidermal keratinocytes

To examine the in vitro cytotoxicity of SCD-153, normal human epidermal keratinocytes (NHEKs) were incubated with increasing concentrations of SCD-153, which revealed time- and dose-dependent cytotoxicity (Fig. 3). Decreased viability was observed at SCD-153 concentrations above 100 μM (Log[Concentration, M] = −4) at 8 hours of incubation and above 10 μM (Log[Concentration, M] = −5) at 16 and 24 hours of incubation. In contrast, both 4-MI and DMI did not cause significant cytotoxicity in NHEKs after 24 hours of incubation across the tested concentrations (0.3 to 500 μM), which may reflect decreased ability of 4-MI and DMI to penetrate cells compared to SCD-153 at the tested concentrations.

The immunomodulatory effects of SCD-153 in sub-cytotoxic conditions were examined by adding SCD-153 in various concentrations to NHEKs that were stimulated with poly I:C or IFNγ, both of which have been suggested to contribute to the pathogenesis

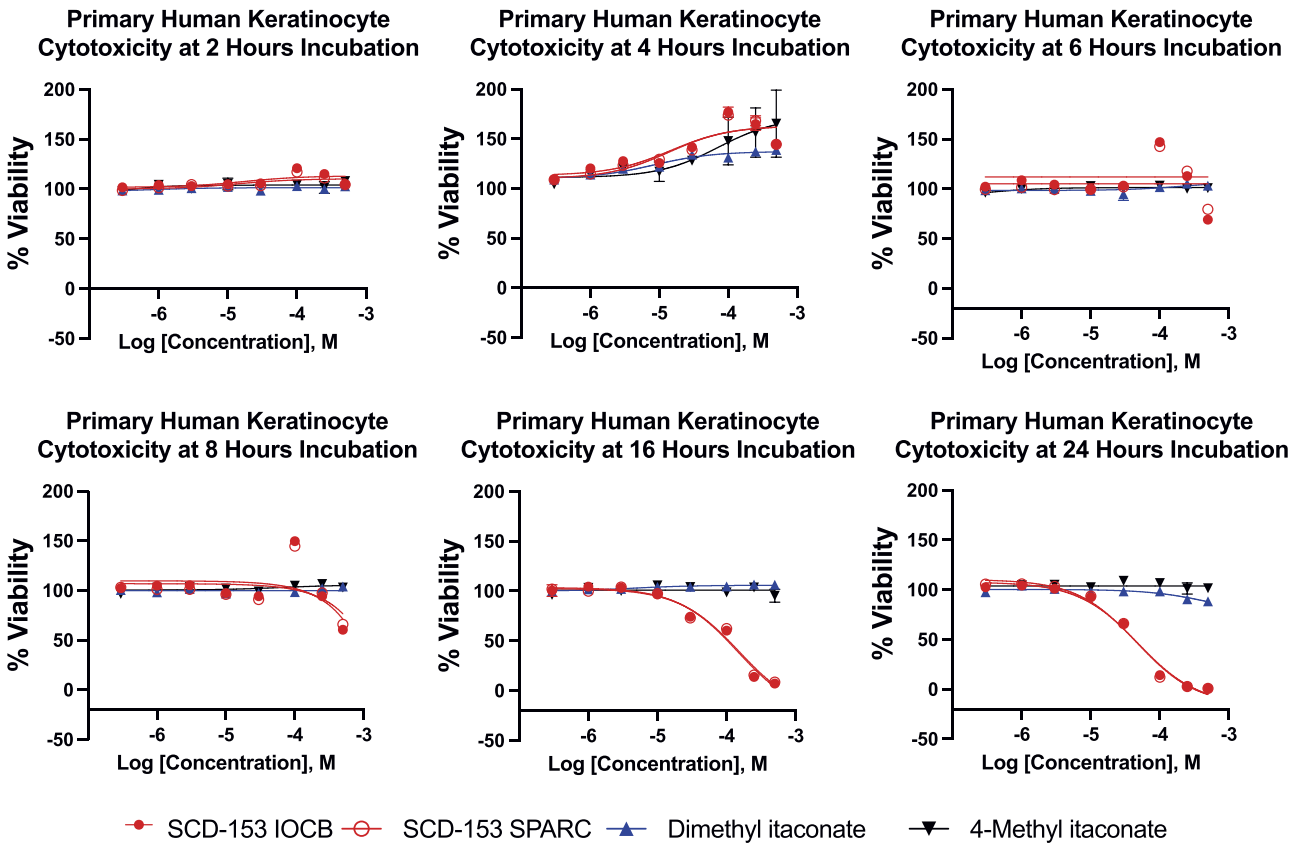

Fig. 3. SCD-153 shows time- and dose-dependent cytotoxicity on NHEKs. Viability (%) of NHEKs incubated with SCD-153, DMI, and 4-MI at various concentrations and durations. NHEKs showed decreased viability after 8 hours of incubation with SCD-153, at drug concentrations above 100 μM ($n = 2$ per compound at each concentration). Separate but chemically identical samples of SCD-153 were prepared at the Institute of Organic Chemistry and Biochemistry (IOCB) and the Sun Pharma Advanced Research Company (SPARC). Data are expressed as mean ± SEM.

of alopecia areata (3, 25–29). In a first set of optimization assays, NHEKs were incubated with poly I:C with or without the presence of SCD-153 for 2, 4, or 8 hours (Fig. 4a). We measured the expression of TLR3 and IL-6, which have been shown to be upregulated by poly I:C in previous studies (34–36). For all three incubation durations that were tested, IL-6 was upregulated by poly I:C and downregulated in a dose-dependent manner by the addition of SCD-153. In contrast, poly I:C-induced upregulation of TLR3 was only seen at 8 hours of incubation and was attenuated with the addition of SCD-153 (Fig. 4a).

Next, we examined changes in the expression of the cytokines IL-6, IL-1β, and IFNβ in NHEKs activated with poly I:C or IFNγ with or without the addition of SCD-153, using an incubation time of 8 hours based on the aforementioned cytotoxicity and optimization studies. SCD-153 caused dose-dependent reduction in poly I:C-induced IL-6, IL-1β, and IFNβ expression, as well as IFNγ-induced IL-6 expression that were statistically significant (Fig. 4b). There were trends of decreased IL-1β expression and increased IFNβ expression with increased SCD-153 concentration in IFNγ-stimulated NHEKs, but these were not statistically significant (Fig. 4b).

SCD-153 accelerates the telogen to anagen transition in C57BL/6 mice with an effect greater than that of 4-MI, DMI, and tofacitinib

The effect of SCD-153 on hair growth in vivo was tested on female C57BL/6 mice aged 8.5 weeks—during the resting (telogen) phase of the hair cycle (37)—similar to experiments with topical JAK inhibitors previously performed by Harel et al (38). We first validated this mouse model by reproducing substantial hair growth with topical 3% or 5% tofacitinib (applied daily for 23 days; Supplementary Material Fig. S1) then proceeded to test SCD-153 under different strengths and dosing regimens with comparisons to 4-MI, DMI, and tofacitinib.

In one experiment, mice were treated on the dorsal right side with vehicle (DMSO), 3% 4-MI, or 3% SCD-153 once every other day on days 1, 3, 5, and 7 after hair clipping, for a total of four doses (Fig. 5a). Mice treated with 3% SCD-153 developed skin erythema and scaling over the days following treatment that were no longer present by day 18, when hair growth occurred consistently. Mice treated with 4-MI showed less skin erythema and scaling but also inconsistent hair growth by day 18 (Fig. 5b and c). Image analysis of photographs showed more than 2-fold greater decrease in mean pixel intensity (suggestive of hair growth and skin darkening) on average in mice treated with 3% SCD-153 compared to 3% 4-MI ($P < 0.05$) and vehicle ($P < 0.05$). While 3% 4-MI induced slightly more hair growth than vehicle on average, the difference between them was not statistically significant ($P = 0.98$) (Fig. 5d).

In another experiment, mice were treated on the dorsal right side with vehicle (DMSO), 40% DMI, 5% tofacitinib, or 5% SCD-153 once every other day on days 1 and 3 after hair clipping, for a total of two doses (Fig. 6a). Like the previous experiment, all mice treated with 5% SCD-153 showed erythema and scaling over the treated areas that were no longer present by day 15, when

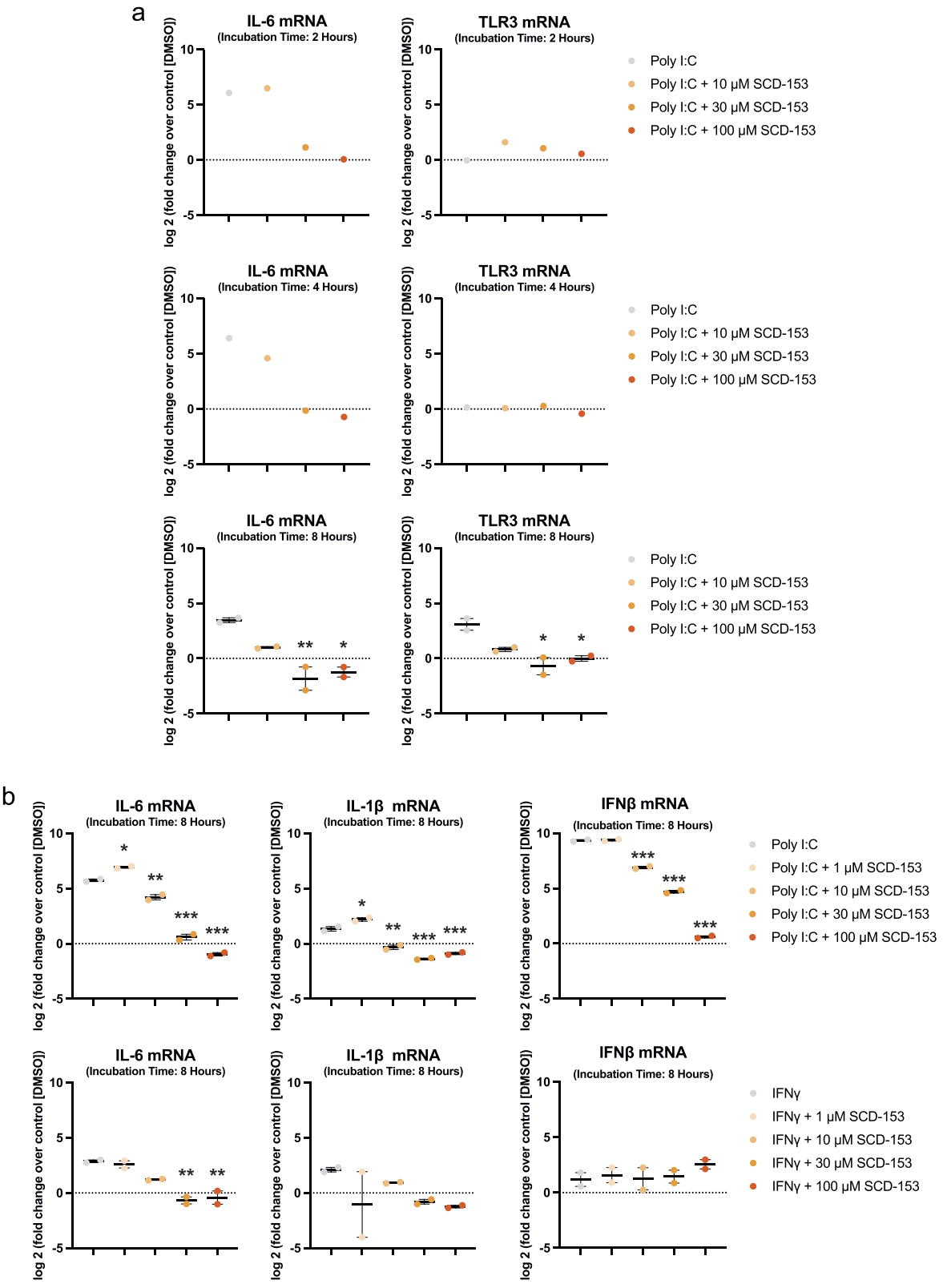

Fig. 4. SCD-153 inhibits poly I:C- and IFNγ- induced expression of proinflammatory cytokines in NHEKs. (a) SCD-153 caused dose-dependent inhibition of poly I:C-induced IL-6 and TLR3 expression in NHEKs at 8 hours of incubation ($n = 2$ per condition for incubation time of 8 hours, $n = 1$ per condition for other incubation times). (b) SCD-153 caused dose-dependent inhibition of poly I:C-induced IL-6, IL-1β, and IFNβ expression and IFNγ-induced IL-6 expression in NHEKs ($n = 2$ per condition). P values were calculated by one-way ANOVA followed by Dunnett's multiple comparisons test. * $P < 0.05$, ** $P < 0.01$, *** $P < 0.001$ compared to poly I:C or IFNγ alone. Data are expressed as mean ± SEM.

a

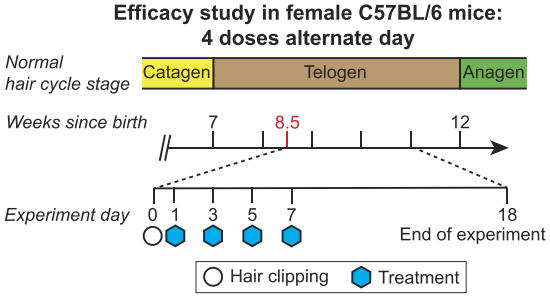

b

Treatment	Strength (%)	n	Erythema/ scaling (day 9)	Hair growth (day 18)	
				Complete	Partial
Vehicle (DMSO), 4 doses alternate day	0	6	0/6	0/6	0/6
4-Methyl itaconate, 4 doses alternate day	3	6	0/6	0/6	2/6
SCD-153 (SPARC), 4 doses alternate day	3	6	6/6	2/6	4/6

c

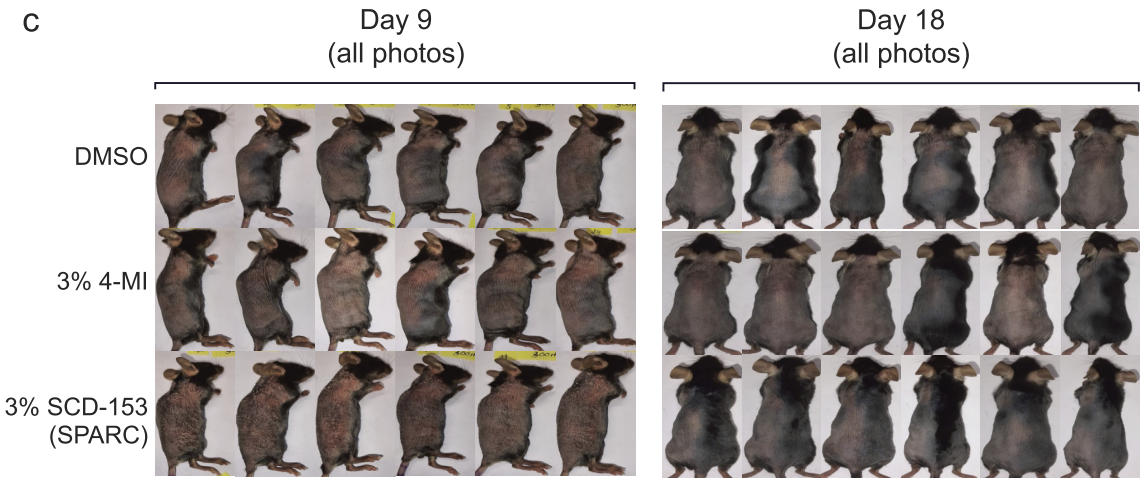

d

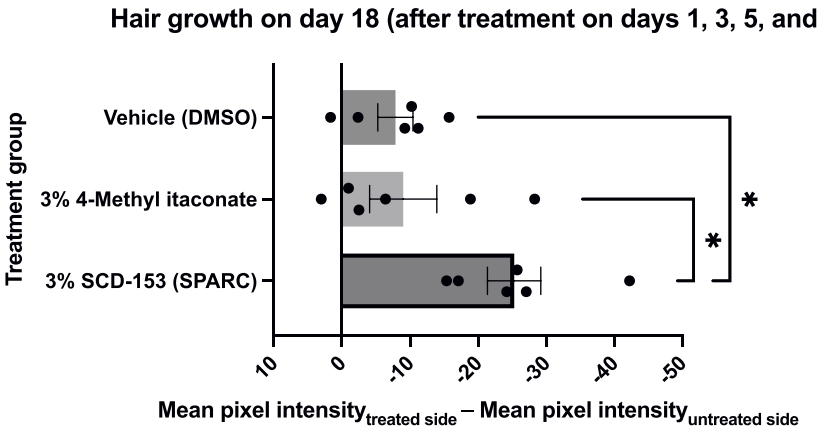

Fig. 5. Topical application of 3% SCD-153 induces early telogen to anagen transition in C57BL/6 mice. (a) Female C57BL/6 mice underwent hair clipping at 8.5 weeks after birth (during the telogen phase of the hair growth cycle), followed by four doses of topical treatment on the dorsal right side with vehicle (DMSO), 3% 4-MI, or 3% SCD-153 on days 1, 3, 5, and 7 after hair clipping. (b) Number and (c) Photographs of mice showing skin erythema and scaling on day 9, as well as hair growth on day 18. (d) Difference in mean pixel intensity between the treated and untreated sides of mice measured from photographs that were converted to 8-bit grayscale images, with negative change in mean pixel intensity suggestive of hair growth and skin darkening. SCD-153 in this experiment was prepared at SPARC. Dots on the bar graph represent measurements of individual mice ($n = 6$ per group). P values were calculated by one-way ANOVA followed by Tukey's multiple comparisons test. * $P < 0.05$. Data are expressed as mean ± SEM.

complete hair growth was consistently observed. Fewer than half of the mice treated with 40% DMI developed skin erythema and scaling, while this was not seen in any mice treated with 5% tofacitinib; however, both 40% DMI and 5% tofacitinib were less consistent in inducing hair growth than 5% SCD-153 (Fig. 6b and c). This was supported by image analysis of photographs, which showed that the average decrease in mean pixel intensity in mice treated with 5% SCD-153 was more than 3-fold greater than both 5% tofacitinib ($P < 0.001$) and 40% DMI ($P < 0.001$) and more than 5.5-fold greater than vehicle ($P < 0.001$). Despite notable hair growth in some mice treated with 40% DMI and 5% tofacitinib, neither agent showed statistically significant hair growth over vehicle on average ($P = 0.65$ and $P = 0.55$, respectively) (Fig. 6d).

Discussion

In this preclinical study, we showed that the novel topical prodrug SCD-153 converts to 4-MI upon penetrating the skin barrier with minimal systemic absorption. While SCD-153 readily metabolizes to 4-MI in skin homogenate (Fig. 1), particularly after

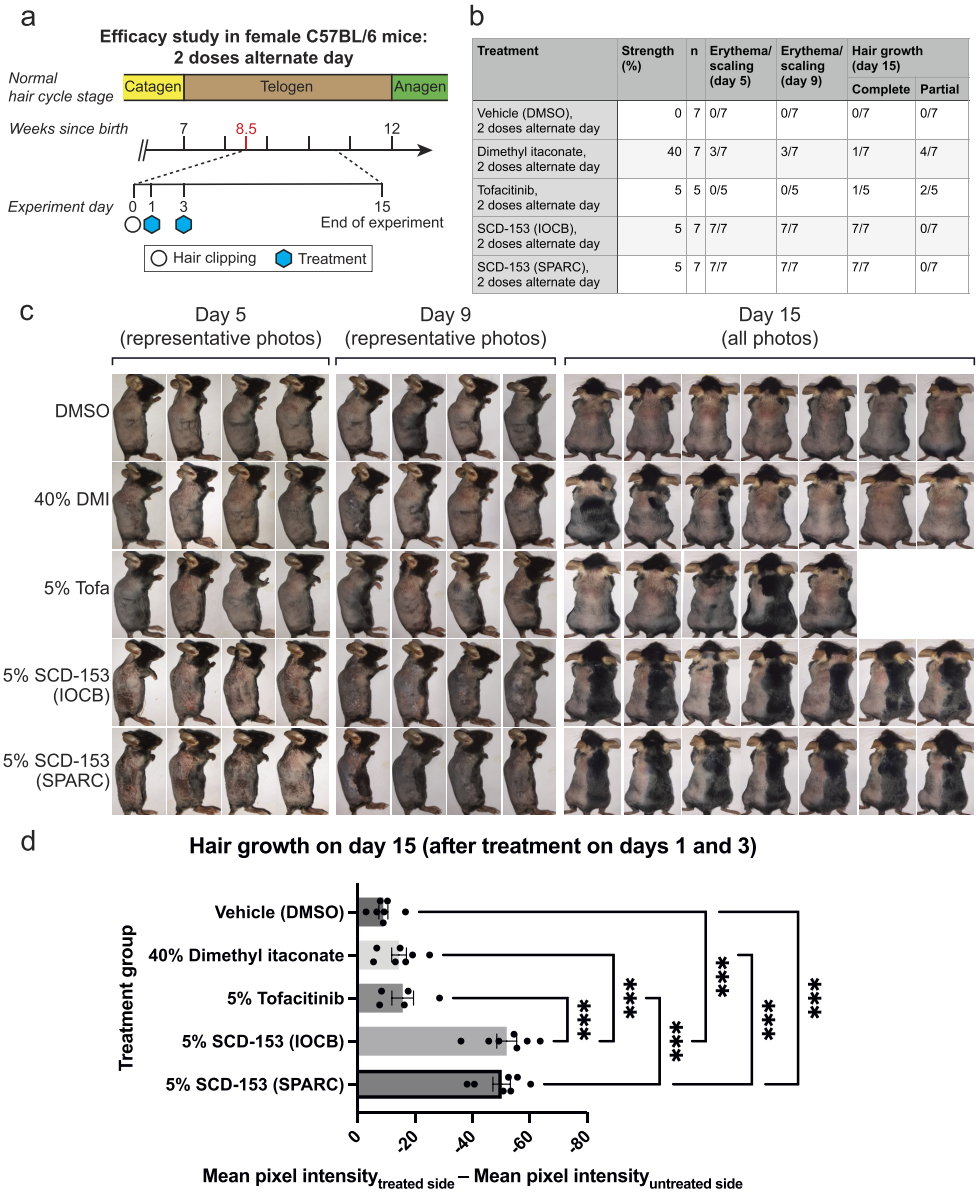

Treatment	Strength (%)	n	Erythema/ scaling (day 5)	Erythema/ scaling (day 9)	Hair growth (day 15)	
					Complete	Partial
Vehicle (DMSO), 2 doses alternate day	0	7	0/7	0/7	0/7	0/7
Dimethyl itaconate, 2 doses alternate day	40	7	3/7	3/7	1/7	4/7
Tofacitinib, 2 doses alternate day	5	5	0/5	0/5	1/5	2/5
SCD-153 (IOCB), 2 doses alternate day	5	7	7/7	7/7	7/7	0/7
SCD-153 (SPARC), 2 doses alternate day	5	7	7/7	7/7	7/7	0/7

Fig. 6. Topical application of 5% SCD-153 induces early telogen to anagen transition in C57BL/6 mice. (a) Female C57BL/6 mice underwent hair clipping at 8.5 weeks after birth (during the telogen phase of the hair growth cycle), followed by two doses of topical treatment on the dorsal right side with vehicle (DMSO), 40% dimethyl itaconate, 5% tofacitinib, or 5% SCD-153 on days 1 and 3 after hair clipping. (b) Number and (c) Photographs of mice showing skin erythema and scaling on days 5 and 9, as well as hair growth on day 15. (d) Difference in mean pixel intensity between the treated and untreated sides of mice measured from photographs that were converted to 8-bit grayscale images, with negative change in mean pixel intensity suggestive of hair growth and skin darkening. Separate but chemically identical samples of SCD-153 were prepared at the IOCB and SPARC. Dots on the bar graph represent measurements of individual mice ($n = 5$ for 5% tofacitinib group, $n = 7$ for all other groups). *P* values were calculated by one-way ANOVA followed by Tukey's multiple comparisons test. *** $P < 0.001$. Data are expressed as mean ± SEM.

penetrating the stratum corneum to enter the rest of the epidermis and dermis (Fig. 2), the lack of a cytotoxic response of 4-MI when incubated with human epidermal keratinocytes even at the highest examined drug concentrations (Fig. 3) suggests that 4-MI may not penetrate cells sufficiently to accumulate toward cytotoxic levels. In this regard, the majority 4-MI recovered from experimental assays was likely the result of intracellular conversion of SCD-153 to 4-MI. Consistent with our objective, we have discovered and synthesized a skin- and cell-permeable derivative of 4-MI that is suitable for topical application.

We used both in vitro and in vivo studies to demonstrate the therapeutic potential of SCD-153 as a topical treatment for hair loss. We showed the ability of SCD-153 to downregulate proinflammatory cytokines in human epidermal keratinocytes in vitro, including IL-6, a known stimulator of JAK-STAT signaling (30), as well as IL-1β, which inhibits hair growth and is elevated in alopecia areata scalp lesions (31–33). We also demonstrated that SCD-153 consistently induces early telogen to anagen transition and significantly more hair growth in C57BL/6 mice than vehicle (DMSO), the less cell-permeable itaconate analogues 4-MI and DMI, and the JAK inhibitor tofacitinib. Our finding that 5% SCD-153 induces greater and more consistent hair growth than 5% tofacitinib in mice when applied using the same dosing regimen (two doses on alternate days) may arise from differences in their mechanism of action and pharmacokinetics of skin penetration. Although topical tofacitinib and ruxolitinib both induce

hair growth in mice (3, 38), they have shown limited efficacy for treating alopecia areata in human trials, likely due to poor skin penetration (11, 12, 39). Insufficient skin penetration may also explain the lack of improvement in alopecia areata treated with topical tacrolimus (FK506) (40), another topical immunosuppressant, despite its theoretical benefit of restoring the immune privilege of hair follicles by downregulating class I major histocompatibility complex proteins (2). In contrast, SCD-153 was chemically designed for topical application to human skin, and its efficacy for stimulating hair growth in mice in this study supports its further investigation in human participants. Besides examining the clinical efficacy of SCD-153 for treating alopecia areata, it would be important to see whether skin erythema and scaling after SCD-153 application also occur in humans, whose epidermis is structurally thicker and more resilient than that of mice.

The presence of skin erythema and scaling after topical application of SCD-153 to mice in this study was unexpected and raises the question of whether they may be related to subsequent hair growth. De novo formation of hair follicles after full-thickness excisional skin wounding, also known as wound-induced hair neogenesis (WIHN), is well-documented in rabbits and mice (41–43). As there have only been few reports of WIHN in humans to date (44–47), the hair growth in mice in this study may not be reproducible in humans if it resulted from cutaneous wounds, rather than the intended pharmacologic effect of SCD-153. However, there are several reasons that hair growth in mice after SCD-153 treatment did not involve WIHN. WIHN occurs with full-thickness skin wounds greater than 1 cm^2 (41, 42), while the skin lesions observed in this study were predominantly small and superficial. New hair from WIHN lack pigmentation and arise in the center of wounds (41, 42), while hair shafts induced by SCD-153 in mice were black and distributed throughout the entire treated area, even in areas without erythema or scaling prior to hair growth. On the molecular level, WIHN requires signaling through the TLR3/IL-6/STAT3 axis, with significantly reduced hair follicle formation upon treatment of wounded mice with the JAK2/STAT3 inhibitor, cucurbitacin I (34). The fact that SCD-153 inhibits TLR3 and IL-6 expression in vitro suggests that it may also suppress WIHN and that hair growth in mice after SCD-153 treatment likely resulted at least in part from a downstream reduction in JAK-STAT signaling (38).

Despite showing that SCD-153 inhibits poly I:C and IFNγ-induced expression of proinflammatory cytokines in NHEKs and promotes early telogen to anagen transition in C57BL/6 mice, this study did not establish a causal relationship between the modulation of cytokines and hair growth. It would be important to clarify the mechanisms of itaconate-based molecules in the context of alopecia areata in future studies through silencing of candidate cytokines or their receptors that may mediate hair growth-promoting effects. The discovery by Runtsch et al. that itaconate and 4-OI inhibit JAK1 protein activity also raises the question of whether SCD-153 may directly modulate JAK-STAT signaling in addition to upstream molecules like TLR3 and IL-6. Finally, the extent to which SCD-153 and 4-MI independently contribute to immunomodulation and hair growth also requires further elucidation. The absence of de-esterified itaconate release by SCD-153 in mouse and human skin homogenate in this study (Table S1) support prior observations that itaconate derivatives like DMI and 4-OI do not undergo de-esterification intracellularly to form itaconate (21, 23, 48). Future studies may examine whether SCD-153 and 4-MI impact intracellular itaconate levels within intact cells either through de-esterification or regulation of endogenous itaconate production.

The mRNA expressions of some cytokines of interest (e.g,. IL-1β) were only modestly upregulated with poly I:C and IFNγ in NHEKs, and our study was limited by the lack of examination of cytokine secretion using an enzyme-linked immunosorbent assay. Although Bambouskova et al. previously showed that DMI may suppress IκBζ induction in vitro in mouse and human primary keratinocytes (20), immune cells—especially macrophages—remain the most well-characterized targets of itaconate (14) and may exhibit greater responses than keratinocytes. In follow-up to the results of this study, we plan to study the effects of SCD-153 on additional cell types involved in the pathogenesis of alopecia areata, such as outer root sheath cells, macrophages, and T lymphocytes. 4-OI has been observed to inhibit mast cell activity in vitro (49), and future studies may examine whether SCD-153 may also modulate abnormal mast cell activity in alopecia areata (50). The suppression of poly I:C-induced IFNβ expression by SCD-153 in this study is similar to that seen with 4-OI in a prior study by Mills et al (19) and warrants characterization in additional contexts, such as in plasmacytoid dendritic cells, which secrete type I IFNs (e.g., IFNα and IFNβ) when activated and have recently been implicated in the pathogenesis of alopecia areata (51, 52).

As the first study to investigate itaconate derivatives for treating hair loss, our results support their continued investigation as a treatment for alopecia areata. Besides initiating human studies, performing studies in C3H/HeJ or humanized mouse models of alopecia areata (53) may further determine the utility of itaconate-based drugs for this condition. Hair cycling and growth involves interactions between multiple cell types and structures, such as hair follicle stem cells, dermal papilla cells, dermal sheath cells, immune cells, adipose tissue, nerves, and vasculature. The extent to which itaconate derivatives may influence these individual components within the structurally complex and dynamic hair follicle niche is an intriguing question that will help to clarify the efficacy and side effects of this emerging class of compound. The development of an effective topical treatment for severe alopecia areata would benefit many patient populations, such as patients with localized alopecia areata, those requiring long-term maintenance after systemic treatment (12), as well as pediatric patients, who may not tolerate corticosteroid injections and tend to have a poorer prognosis (5, 54). While this study focused on the topical application of an itaconate analogue, future investigations may explore other routes of administration to target hair follicles, such as intralesional injection, laser-assisted drug delivery, and microneedle arrays.

Materials and Methods

Study Approval

All animal studies were conducted in accordance with protocols reviewed and approved by the Institutional Animal Care and Use Committee of Johns Hopkins University or Institutional Animal Ethics Committee of SPARC. Animals were housed in Association for Assessment and Accreditation of Laboratory Animal Care (AALAC)-approved facilities in compliance with the Public Health Service Policy on the Humane Care and Use of Laboratory Animals or Committee for the Purpose of Control and Supervision of Experiments on Animals (CPCSEA) guidelines.

Synthesis of itaconate prodrug

The itaconate prodrug, SCD-153, was synthesized by the reaction of 4-MI (CAS: 7338–27–4) with chloromethyl isopropyl carbonate

in the presence of potassium carbonate and either acetonitrile or acetone as the solvent, as illustrated in Fig. 1a and further described in the Supplementary Methods. The structure and purity of SCD-153 were confirmed using liquid chromatography with $^{1}H/^{13}C$ nuclear magnetic resonance spectroscopy, high-resolution mass spectrometry, and elemental analysis. Separate samples of SCD-153 were synthesized at the IOCB of the Czech Academy of Sciences and SPARC. Calculated logarithm of partition coefficient (CLogP) values of SCD-153 and 4-MI were obtained using ChemDraw 20.1 (PerkinElmer Inc., Waltham, MA, USA). Additional procedural and analytical measurements of SCD-153 are provided in the Supplementary Methods.

Solid state stability of SCD-153

Solid SCD-153 was incubated at room temperature for 1, 2, 3, 4, 7, 14, 21, 28, 63, and 84 days. On the day of analysis, each sample was dissolved in DMSO to make a 100 mM stock solution, which was further diluted to 10 μM in methanol for analysis using liquid chromatography-mass spectrometry (LC-MS). Samples were analyzed on an Agilent 1290 HPLC coupled to Agilent 6520B QTOF equipped with ESI Dual source (Agilent Technologies, Santa Clara, CA, USA). SCD-153 was resolved on an Agilent EclipsePlus C18 RRHD (1.8 μm) 2.1 × 100 mm column. The mobile phase consisted of LC–MS grade water + 0.1% formic acid (A) and acetonitrile + 0.1% formic acid (B). Separation was achieved using a gradient run at a flow rate of 0.4 mL/minute. The mass spectrometer was operated in a positive ion mode at 350°C with drying gas and nebulizer set at 40 psig. Mass spectrometry data were analyzed with the MassHunter Quantitative Analysis software (Agilent Technologies, Santa Clara, CA, USA).

Metabolic stability of SCD-153 in plasma and skin homogenates

The metabolic stability of SCD-153 was assessed in mouse skin homogenate, mouse plasma, human skin homogenate, and human plasma. Skin homogenates were prepared by 10-fold dilution of washed skin samples in 0.1 M potassium phosphate buffer followed by homogenization with a probe sonicator. 1 mL aliquots of mouse skin homogenate, human skin homogenate, CD1 mouse plasma, and human plasma were spiked with SCD-153 to a concentration of 20 μM, followed by incubation in an orbital shaker at 37°C. All stability studies were conducted at predetermined time points (0, 30, and 60 minutes), when 10 μL aliquots of the mixture were removed in triplicate and quenched by the addition of 50 μL of ice-cold acetonitrile containing internal standard (losartan: 0.5 μM). The samples were vortex-mixed for 30 seconds and centrifuged at 10,000 g for 10 minutes at 4°C. Supernatants were transferred to a 96-well plate and analyzed using high-resolution mass spectrometer. Levels of SCD-153, 4-MI, and itaconate were monitored over time using the same bioanalysis methods described in the preceding solid state stability section.

Pharmacokinetics of SCD-153 following topical application in mice

C57BL/6 mice with 16 to 22 g weight range and 8 to10 weeks of age were maintained on a 12-hour light-dark cycle, with access to food and water, ad libitum. The mice were shaved and treated topically with 5% SCD-153 in DMSO on half of the dorsal back, then anesthetized with isoflurane inhalation at predetermined time points. Blood samples were collected in heparinized microtubes and centrifuged (8500 rpm for 7 minutes); plasma was collected in polypropylene tubes and stored at –70°C. To prevent ex vivo degradation of SCD-153, plasma samples were stabilized with 2% formic acid prepared in deionized water (plasma:stabilizer volume ratio—2:1).

For the collection of skin samples, application sites were washed with cotton swabs and collected in prelabelled sampling tubes. Ten same-size cotton swabs pre-soaked in 1 mL of 0.1% formic acid in water:acetonitrile (30:70% v/v) were used to wash the application site. An additional dry cotton swab was used to further dry the application site. In experiments that involved separation of the stratum corneum, tape stripping of skin was performed five times using Micropore surgical tape (3M India Limited, Bengaluru, India) to remove the stratum corneum. The skin (with or without removal of stratum corneum with tape stripping) was dissected from the application site, washed with ice-cold phosphate-buffered saline, gently dried on blotting paper, and snap frozen in liquid nitrogen. Strip and skin samples were weighed and immersed in 0.1% formic acid in water:acetonitrile (30:70% v/v). All study samples were stored in deep freezer at –70°C until bioanalysis.

For bioanalysis in pharmacokinetic studies, blank matrix (plasma, homogenized tape strips and skin) fortified with stabilizer (2% formic acid) were spiked with appropriate concentrations of SCD-153 and 4-MI to obtain standards (5 to 2500 ng/mL for SCD-153 and 50 to 10,000 ng/mL for 4-MI) and quality controls (15 to 2000 ng/mL for SCD-153 and 150 to 7500 ng/mL for 4-MI). 100 μL of study samples were precipitated with 0.5 mL of 0.1% formic acid in acetonitrile containing 500 ng/mL of tolbutamide and vortexed for 5 minutes, followed by centrifugation at 10,000 rpm for 10 minutes at 10°C. The supernatant was directly injected to LC-MS/MS system to quantify SCD-153 and 4-MI, as described below.

A simultaneous chromatographic analysis was performed using an Acquity Ultra-High Performance System consisting of an analytical pump and an auto sampler coupled with API 4000 mass spectrometer. Separation of analyte was achieved at 40°C temperature using HyPURITY C18 column (100 mm × 2.1 mm i.d., 5 μ). The mobile phase consisted of acetonitrile and 0.1% formic acid in 5 mm ammonium format with gradient elution. SCD-153 and 4-MI were monitored using ion transitions m/z 261.1 → 127.100 and m/z 145.1 → 113.100, respectively. The internal standard (tolbutamide) was monitored using ion transition m/z 271.1 → 91.100.

Human eidermal keratinocyte cytotoxicity

NHEKs (Lonza, Basel, Switzerland) were revived, allowed to expand, and seeded in 96-well plates. SCD-153, DMI, and 4-MI were diluted to concentrations of 500, 250, 100, 30, 10, 3, 1, and 0.3 μM and added to the assay plates containing NHEKs. The plates were checked for compound effects after 2, 4, 6, 8, 16, and 24 hours of incubation to determine % viability of NHEKs. Cell viability was measured with CellTiter-Glo assay (Promega, Madison, WI, USA).

Gene expression profiles of human eidermal keratinocytes

NHEKs were seeded in plates and incubated overnight at 37°C and 5% CO_2, followed by stimulation with poly I:C (50 μg/mL) or IFNγ (5 ng/mL) with or without the presence of SCD-153 at the concentrations of 1, 10, 30, or 100 μM. RNA was isolated and analyzed with TaqMan RT-PCR (Thermo Fisher Scientific, Waltham, MA, USA) to quantify fold changes in the expression of genes of interest, including IL-6, TLR3, IL-1β, and IFNβ.

Mouse efficacy studies

Female C57BL/6 mice (inbred at SPARC, breeder pair strain: C57BL/6NCrl) were used to study hair growth due to their well-characterized hair growth cycle, with a prolonged telogen phase compared to male mice suitable for studying factors that promote the telogen to anagen transition (37). All mice underwent complete hair removal on the dorsal side with a clipper at 8.5 weeks after birth, during the telogen phase of the murine hair growth cycle (37). The mice subsequently received topical treatments with different dosing regimens. In the "4 doses alternate day" regimen, the mice received topical treatment with 150 μL of vehicle (DMSO), 3% 4-MI, or 3% SCD-153 on the dorsal right side once every other day on days 1, 3, 5, and 7 after hair clipping, for a total of four treatments. In the "2 doses alternate day" regimen, the mice received topical treatment with 150 μL of vehicle (DMSO), 40% DMI, 5% tofacitinib, or 5% SCD-153 on the dorsal right side once every other day on days 1 and 3 after hair clipping, for a total of two treatments. The dorsal left side was not treated in all mice. Photographs were taken for the evaluation of skin reactions and hair growth.

Image analysis of hair growth

Photographs of mice were analyzed with ImageJ (Fiji) version 1.53f51 to quantify hair growth. Photographs were converted to grayscale 8-bit images, with the intensity of each pixel ranging from 0 (black) to 255 (white). To reduce evaluator bias, the file names of all photographs were randomized prior to image analysis. For each photograph, the dorsal right (treated) and dorsal left (untreated) sides of mice were manually outlined with the polygon selection tool, and the mean pixel intensity of both regions was measured. The difference in mean pixel intensity between the treated and untreated sides was used to represent hair growth attributable to treatment, with negative change in mean pixel intensity suggestive of hair growth and skin darkening.

Statistical analysis

Statistical analyses and visualizations were performed with GraphPad Prism 9 (GraphPad Software Inc., San Diego, CA, USA) and Microsoft Excel (Microsoft Corporation, Redmond, WA, USA). Two-sided $P < 0.05$ was regarded as statistically significant.

Acknowledgment

We thank Deependrakumar Singh and Ankit Bhatt for their support during the in-life phase of dermal pharmacokinetic studies in mice.

Supplementary Material

Supplementary material is available at *PNAS Nexus* online.

Funding

This research was supported by NIH/NCATS UL1 TR003098 (BSS), NIH/NIAMS R01 AR068280 and AR064297 (LAG), Maryland Innovation Initiative (BSS, LAG, RR), and the Institute of Organic Chemistry and Biochemistry of the Academy of Sciences of the Czech Republic, v.v.i. (PM, IS).

Authors' Contributions

Wrote manuscript: Tsai, Gori, Nigade, Snajdr, Majer, Rais, Slusher, and Garza.
Designed research: Iyer, Talwar, Sutariya, Jani, Venkatasubbaiah, Nigade, Talluri, Murty, Ramanathan, Li, Islam, Majer, and Rais, Garza.
Performed research: Gori, Alt, Tiwari, Hinsu, Ahirwar, Mohanty, Khunt, Sutariya, Jani, Patel, Meghapara, Sahu, Rana, Nigade, Kiritkumar Joshi, Li, Islam, Snajdr, and Garza.
Analyzed data: Tsai, Alt, Iyer, Sutariya, Jani, Venkatasubbaiah, Kaushal Joshi, Nigade, Murty, Ramanathan, Rais, and Garza.

Data Availability

The data discussed in this manuscript are available on Mendeley Data at http://dx.doi.org/10.17632/shsh37w4sg.1.

References

1. Lee HH, *et al.* 2020. Epidemiology of alopecia areata, ophiasis, totalis, and universalis: a systematic review and meta-analysis. J Am Acad Dermatol. 82(3):675–682.
2. Bertolini M, Mcelwee K, Gilhar A, Bulfone-Paus S, Paus R. 2020. Hair follicle immune privilege and its collapse in alopecia areata. Exp Dermatol. 29(8):703–725.
3. Xing L, *et al.* 2014. Alopecia areata is driven by cytotoxic T lymphocytes and is reversed by JAK inhibition. Nat Med. 20(9):1043–1049.
4. Strazzulla LC, *et al.* 2018. Alopecia areata: disease characteristics, clinical evaluation, and new perspectives on pathogenesis. J Am Acad Dermatol. 78(1):1–12.
5. Tosti A, Bellavista S, Iorizzo M. 2006. Alopecia areata: a long term follow-up study of 191 patients. J Am Acad Dermatol. 55(3):438–441.
6. Meah N, *et al.* 2021. The alopecia areata consensus of experts (ACE) study part II: results of an international expert opinion on diagnosis and laboratory evaluation for alopecia areata. J Am Acad Dermatol. 84(6):1594–1601.
7. Okhovat J-P, *et al.* 2019. Association between alopecia areata, anxiety, and depression: a systematic review and meta-analysis. J Am Acad Dermatol. 10.1016/j.jaad.2019.05.086
8. Liu LY, King BA, Craiglow BG. 2016. Health-related quality of life (HRQoL) among patients with alopecia areata (AA): a systematic review. J Am Acad Dermatol. 75(4):806–812.e3.
9. Strazzulla LC, *et al.* 2018. Alopecia areata: an appraisal of new treatment approaches and overview of current therapies. J Am Acad Dermatol. 78(1):15–24.
10. Vandiver A, Girardi N, Alhariri J, Garza LA. 2017. Two cases of alopecia areata treated with ruxolitinib: a discussion of ideal dosing and laboratory monitoring. Int J Dermatol. 56(8):833–835.
11. Phan K, Sebaratnam DF. 2019. JAK inhibitors for alopecia areata: a systematic review and meta-analysis. J Eur Acad Dermatol Venereol. 33(5):850–856.
12. Wang EHC, Sallee BN, Tejeda CI, Christiano AM. 2018. JAK inhibitors for treatment of alopecia areata. J Invest Dermatol. 138(9):1911–1916.
13. Gilhar A, Keren A, Paus R. 2019. JAK inhibitors and alopecia areata. Lancet North Am Ed. 393(10169):318–319.
14. O'Neill LAJ, Artyomov MN. 2019. Itaconate: the poster child of metabolic reprogramming in macrophage function. Nat Rev Immunol. 19(5):273–281.

15. Strelko CL, *et al.* 2011. Itaconic acid is a mammalian metabolite induced during macrophage activation. J Am Chem Soc. 133(41):16386–16389.
16. Lampropoulou V, *et al.* 2016. Itaconate links inhibition of succinate dehydrogenase with macrophage metabolic remodeling and regulation of inflammation. Cell Metab. 24(1):158–166.
17. Peace CG, O'Neill LAJ. 2022. The role of itaconate in host defense and inflammation. J Clin Invest. 132(2):e148548. 10.1172/jci148548
18. Lin J, Ren J, Gao DS, Dai Y, Yu L. 2021. The emerging application of Itaconate: promising molecular targets and therapeutic opportunities. Front Chem. 9:669308.
19. Mills EL, *et al.* 2018. Itaconate is an anti-inflammatory metabolite that activates Nrf2 via alkylation of KEAP1. Nature. 556(7699):113–117.
20. Bambouskova M, *et al.* 2018. Electrophilic properties of itaconate and derivatives regulate the iκbζ–ATF3 inflammatory axis. Nature. 556(7702):501–504.
21. Swain A, *et al.* 2020. Comparative evaluation of itaconate and its derivatives reveals divergent inflammasome and type I interferon regulation in macrophages. Nat Metab. 2(7): 594–602.
22. Hooftman A, *et al.* 2020. The immunomodulatory metabolite itaconate modifies NLRP3 and inhibits inflammasome activation. Cell Metab. 32(3):468–478 e7.
23. He W, *et al.* 2022. Mesaconate is synthesized from itaconate and exerts immunomodulatory effects in macrophages. Nat Metab. 4(5):524–533.
24. Hooftman A, O'Neill LAJ. 2019. The immunomodulatory potential of the metabolite itaconate. Trends Immunol. 40(8): 687–698.
25. Shin J-M, *et al.* 2017. Double-stranded RNA induces inflammation via the NF-κB pathway and inflammasome activation in the outer root sheath cells of hair follicles. Sci Rep. 7(1):44127.
26. Shin J-M, *et al.* 2018. Induction of alopecia areata in C3H/HeJ mice using polyinosinic-polycytidylic acid (poly[I:C]) and interferon-gamma. Sci Rep. 8(1). 12518. doi: 10.1038/s41598-018-30997-3.
27. Mcphee CG, *et al.* 2012. Increased expression of Cxcr3 and its ligands, Cxcl9 and Cxcl10, during the development of alopecia areata in the mouse. J Invest Dermatol. 132(6):1736–1738.
28. Glickman JW, *et al.* 2021. Cross-sectional study of blood biomarkers of patients with moderate to severe alopecia areata reveals systemic immune and cardiovascular biomarker dysregulation. J Am Acad Dermatol. 84(2):370–380.
29. Pratt CH, King LE, Messenger AG, Christiano AM, Sundberg JP. 2017. Alopecia areata. Nat Rev Dis Primers. 3(1):17011.
30. Heinrich PC, *et al.* 2003. Principles of interleukin (IL)-6-type cytokine signalling and its regulation. Biochem J. 374(1):1–20.
31. Hoffmann R. 1999. The potential role of cytokines and T cells in alopecia areata. J Investig Dermatol Symp Proc. 4(3): 235–238.
32. Hoffmann R, Eicheler W, Wenzel E, Happle R. 1997. Interleukin-1beta-induced inhibition of hair growth in vitro is mediated by cyclic AMP. J Invest Dermatol. 108(1):40–42.
33. Hoffmann R, *et al.* 1994. Cytokine mRNA levels in Alopecia areata before and after treatment with the contact allergen diphenylcyclopropenone. J Invest Dermatol. 103(4):530–533.
34. Nelson AM, *et al.* 2015. dsRNA released by tissue damage activates TLR3 to drive skin regeneration. Cell Stem Cell. 17(2):139–151.
35. Prens EP, *et al.* 2008. IFN-α enhances poly-IC responses in Human keratinocytes by inducing expression of cytosolic innate RNA receptors: relevance for psoriasis. J Invest Dermatol. 128(4):932–938.
36. Kalali BN, *et al.* 2008. Double-stranded RNA induces an antiviral defense status in epidermal keratinocytes through TLR3-, PKR-, and MDA5/RIG-I-Mediated differential signaling. J Immunol. 181(4):2694–2704.
37. Müller-Röver S, *et al.* 2001. A comprehensive guide for the accurate classification of murine hair follicles in distinct hair cycle stages. J Invest Dermatol. 117(1):3–15.
38. Harel S, *et al.* 2015. Pharmacologic inhibition of JAK-STAT signaling promotes hair growth. Sci Adv. 1(9):e1500973.
39. Hosking AM, Juhasz M, Mesinkovska NA. 2018. Topical Janus kinase inhibitors: a review of applications in dermatology. J Am Acad Dermatol. 79(3):535–544.
40. Price VH, Willey A, Chen BK. 2005. Topical tacrolimus in alopecia areata. J Am Acad Dermatol. 52(1):138–139.
41. Wier EM, Garza LA. 2020. Through the lens of hair follicle neogenesis, a new focus on mechanisms of skin regeneration after wounding. Semin Cell Dev Biol. 100:122–129.
42. Ito M, *et al.* 2007. Wnt-dependent de novo hair follicle regeneration in adult mouse skin after wounding. Nature. 447(7142):316–320.
43. Billingham RE, Russell PS. 1956. Incomplete wound contracture and the phenomenon of hair neogenesis in rabbits' Skin. Nature. 177(4513):791–792.
44. Kligman AM, Strauss JS. 1956. The formation of vellus hair follicles from human adult epidermis. J Invest Dermatol. 27(1):19–23.
45. Sun Z, Diao J, Guo S, Yin G. 2009. A very rare complication: new hair growth around healing wounds. J Int Med Res. 37(2): 583–586.
46. Beachkofsky TM, Henning JS, Hivnor CM. 2011. Induction of de novo hair regeneration in scars after fractionated carbon dioxide laser therapy in three patients. Dermatol Surg. 37(9): 1365–1368.
47. Wong T-W, Hughes M, Wang S-H. 2018. Never too old to regenerate? Wound induced hair follicle neogenesis after secondary intention healing in a geriatric patient. J Tissue Viability. 27(2):114–116.
48. Elazzouny M, *et al.* 2017. Dimethyl itaconate is not metabolized into itaconate intracellularly. J Biol Chem. 292(12):4766–4769.
49. Hu B, Zhao S, Huang M, Ren J. 2020. Nuclear factor E2 related factor (NRF2) inhibits mast cell- mediated allergic inflammation via SIRT4-mediated mitochondrial metabolism. Ann Palliat Med. 9(6):3839–3847.
50. Bertolini M, *et al.* 2014. Abnormal interactions between perifollicular mast cells and CD8+ T-Cells may contribute to the pathogenesis of alopecia areata. PLoS One. 9(5):e94260.
51. Abou Rahal J, Kurban M, Kibbi AG, Abbas O. 2016. Plasmacytoid dendritic cells in alopecia areata: missing link? J Eur Acad Dermatol Venereol. 30(1):119–123.
52. Saadeh D, Kurban M, Abbas O. 2016. Update on the role of plasmacytoid dendritic cells in inflammatory/autoimmune skin diseases. Exp Dermatol. 25(6):415–421.
53. Gilhar A, Laufer Britva R, Keren A, Paus R. 2020. Mouse models of Alopecia Areata: C3H/HeJ mice versus the humanized AA Mouse model. J Investig Dermatol Symp Proc. 20(1):S11–S15.
54. Messenger AG, *et al.* 2012. British association of dermatologists' guidelines for the management of alopecia areata 2012. Br J Dermatol. 166(5):916–926.